Litho-structural characterization of the Birimian formations of the Chappelle gold deposit (Hiré, southern Fettékro Birimian belt, west-central Côte d'Ivoire): Implications for mineralization and metallogeny

Abstract

The Hiré gold deposit, located in the southern part of the Fettékro Birimian greenstone belt in central-western Côte d'Ivoire, constitutes one of the major Paleoproterozoic gold districts of the West African Craton. This study focuses on the geological, petrographic, structural, and geochemical characterization of the Hiré gold-bearing system in order to constrain the hydrothermal processes controlling gold mineralization and discuss its metallogenic significance. Field investigations, petrographic analyses, and geochemical data reveal that the mineralization is hosted within volcano-sedimentary Birimian formations affected by intense hydrothermal alteration and regional deformation related to the Eburnean orogeny. Gold mineralization is associated with quartz-carbonate veins, disseminated sulfides, silicification, sericitization, chloritization, and carbonate alteration. Structural analyses demonstrate that mineralized zones are mainly controlled by NE-SW and NNW-SSE shear corridors associated with transcurrent tectonics during the Eburnean deformation event. The integration of geological, petrographic, structural, and geochemical data suggests that the Hiré deposit belongs to a mesothermal-orogenic gold system comparable to other Birimian gold provinces of Ghana, Burkina Faso, and Mali.

Keywords: Hiré, Birimian, gold mineralization, hydrothermal alteration, quartz veins, Côte d'Ivoire

1.Introduction

The West African Craton represents one of the most important gold domains in the world thanks to its numerous Paleoproterozoic Birimian greenstone belts rich in orogenic gold deposits (Bessoles, 1977; Milési et al., 1992; Groves et al., 1998). In Côte d'Ivoire, the Fettékro Birimian greenstone belt constitutes a major metallogenic corridor bringing together several major gold deposits such as Hiré, Bonikro, and Dougbafla (Pouclet et al., 2006; Vidal et al., 2009). The Hiré deposit is located in the southern part of the Oumé-Fettékro Birimian belt and exhibits gold mineralization primarily controlled by regional tectonic structures and hydrothermal fluid circulation (Yao et al., 2001).

According to Goldfarb et al. (2001), orogenic gold systems generally develop in compressional tectonic settings associated with deep crustal shear zones. The objective of this study is to characterize the Hiré gold deposit through an integrated approach combining geology, petrography, structural analysis, and metallogenic interpretation.

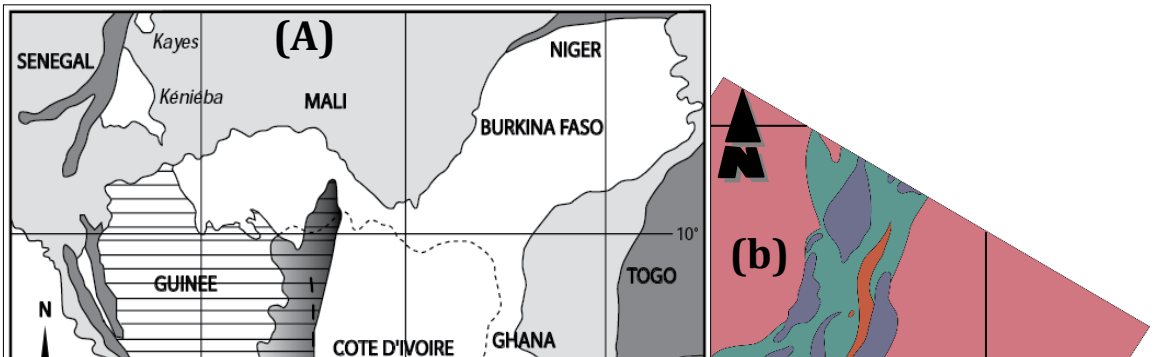
2. Regional and Local Geological Setting

2.1. Geodynamic Framework and Orogenic Evolution

The Hiré gold deposit is integrated into the geological history of the Baoulé-Mossi domain (Lower Proterozoic), a major entity of the West African Craton situated on the Man Ridge (Bessoles, 1977). The structuring of this domain took place during the Eburnean orogenic cycle (2.5 to 1.6 Ga), marked by the emplacement of Birimian formations documented by numerous authors (Arnould, 1961 ; Tagini, 1971 ; Yacé, 1984 ; Boher et al., 1989 ; Feybesse et al., 1989 ; Milési et al., 1989 ; Abouchami, 1990 ; Doumbia et al., 1998).

2.2. Lithostratigraphy of the Hiré District

Locally, the Hiré deposit is hosted primarily within mafic metavolcanic rocks (metabasalts, locally meta-andesites) and metamorphosed volcano-detrital sediments (metatuffs, metagreywackes). These lithologies have undergone low- to medium-grade metamorphism, characterized by mineral assemblages such as actinolite, chlorite, epidote, sericite, and quartz. The region is marked by polyphase deformation, with the development of a regional foliation and ductile shear zones that control the orientation and localization of mineralized bodies. Late-Birimian granitic intrusions are also present in the region, but their direct role in the genesis of the Hiré deposit is not always clearly established.



UNDER PEER REVIEW NUAE

Figure 1: a) Map of the Man Ridge (Bessoles, 1977); (b) Map of the southern part of the Oumé-Fettékro greenstone belt (Yacé, 1976; modified).

2.3. Deformation

The current architecture of the Fettékro belt is the result of several Eburnean tectonic episodes characterized by regional shear corridors oriented NE-SW and NNW-SSE. These shearing structures (Delor et al., 2004) constitute the main structural conduits for hydrothermal fluid circulation and gold trapping.

3. Methodology

The methodology is based on field investigations including a literature review, mapping of geological units and veins, structural surveys, descriptions of hydrothermal alterations, and sampling. Due to a thick lateritic cover (40 to 120 m), the petrographic study relied on macroscopic and microscopic analyses of approximately one hundred drill core samples and rare outcrops. Around thirty thin sections were examined under a polarizing microscope to define textures, mineral relationships, and sulfide assemblages. Finally, the study of the mineralization combined binocular loupe observations, polished sections examined under an ore microscope, and SEM (Scanning Electron Microscopy) analyses at the Centre d'Analyses et de Recherche (CAR) of PETROCI in Côte d'Ivoire to characterize the parageneses.

4. Results4.1. Petrography

The lithologies of the Chappelle deposit are dominated by mafic metavolcanics intruded by granitoids, dioritoids, and felsic dikes.

4.1.1. Mafic Metavolcanics

Mafic metavolcanics form the main backbone of the lower volcanic sequence of the Fettékro Birimian belt in the Hiré district. They crop out mainly as massive flows or locally as pillow lava facies, indicating an original subaqueous effusive volcanism.

On a local scale, these rocks are essentially metabasalts displaying macroscopically a dark green to greenish color (greenstones), an aphanitic to fine-grained texture, and a structure ranging from locally isotropic to strongly foliated near shear corridors (Fig. 2 A).

Thin sections reveal sericitized albite laths and pyroxene phenocrysts pseudomorphosed into chlorite. Under the effect of regional Eburnean metamorphism, the primary mineral assemblage (pyroxene + calcic plagioclase) underwent a recrystallization paragenesis characteristic of the greenschist facies. This assemblage is dominated by the chlorite + epidote + actinolite + albite + calcite association (Fig. 2 B).

Within the envelope of the Hiré deposit, these mafic metavolcanics constitute a preferential host rock for gold mineralization. They are intensely affected by syn-deformational hydrothermal alteration, resulting in diffuse carbonatization, sericitization, and sulfidization (mainly disseminated pyrite) associated with the network of quartz veins and veinlets.

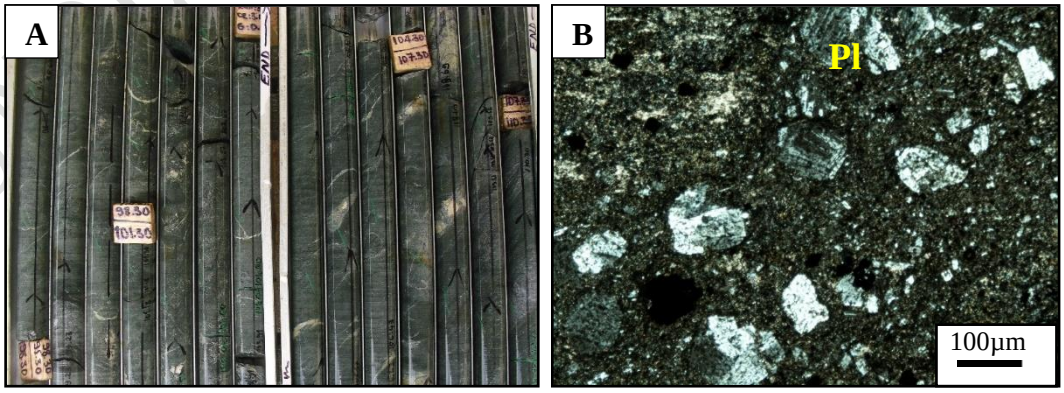


Figure 2: (A) Photograph and (B) photomicrograph of basalt.
Pl: plagioclase

44.1.2. Granitoids

The granitoids encountered are mainly represented by granodiorites, tonalites, and locally biotite granites.

UNDER PEER REVIEW IN IJAR

4.1.2.1. Granodiorite

They generally exhibit a light gray to pinkish-gray color, displaying medium- to coarse-grainedphaneritic textures, and occasionally porphyritic textures with plagioclase megacrysts (Fig. 3 A). Depending on their structural position relative to the shear corridors of the Fettékro belt, these plutons display strongly foliated and stretched margins (syn-tectonic facies) contrasting with isotropic cores preserved from deformation (post-tectonic facies). The rock reacts weakly to a hand magnet, suggesting the presence of minor amounts of magnetite.

In thin section, the primary mineral assemblage combines quartz, plagioclase, potassium feldspar, and biotite, sometimes accompanied by hornblende, as well as secondary chlorite, muscovite, epidote, and sericite resulting from retromorphism in the greenschist facies (Fig. 3 B).

From a metallogenic perspective, the rigid mechanical behavior of these granitoid bodies generated a strong competency contrast with the surrounding ductile Birimian schists. During regional transpressive deformation, this contrast promoted intense brittle-to-ductile fracturing at the margins of the plutons, creating high-permeability zones. In the Hiré deposit sector, hydrothermal fluids exploited these zones of structural weakness, resulting in strong silicification, sericitization, pyritization, and the establishment of auriferous quartz vein networks (sheeted veins) crosscutting the intrusive massifs.

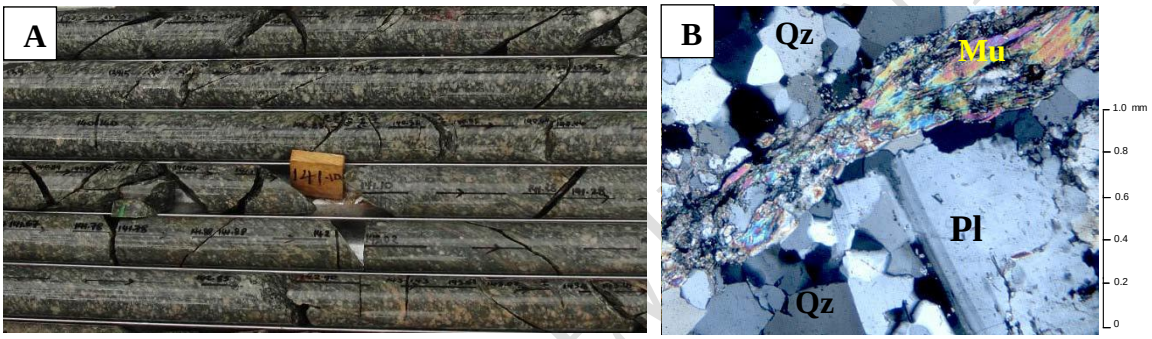


Figure 3: (A) Photograph and (B) photomicrograph of granodiorite
Pl: plagioclase; Qz: quartz; Mu: Muscovite.

4.1.2.2. Tonalite

The mesocratic tonalite was characterized by moderately abundant primary interstitial quartz.

In polished thin section, this sample exhibits a partially preserved igneous texture, severely modified by strong ductile deformation and pervasive alteration effects (Fig. 4 A).

Large plagioclase grains, approximately 3–5 mm in size, are abundant throughout the rock. All are aligned within a strong metamorphic foliation, and all have undergone severe replacement by fine flakes of sericite, some of which are massive while others are aligned parallel to the foliation trace. These are interpreted as large residual primary plagioclase crystals.

Quartz is present in lesser amounts as finer-grained granoblastic mosaics composed of grains approximately 0.2–0.4 mm in size. These quartz aggregates are strongly elongated parallel to the foliation trace as lenses and lenticles. In places, the less deformed zones appear to partially enclose the large plagioclase crystals, suggesting that the quartz originally formed as interstitial igneous quartz grains (Fig. 4 B).

A fine-grained foliated matrix encloses the large plagioclase grains. It is composed of small anhedral plagioclase grains forming a microgranular mosaic texture, accompanied principally by fine-grained trails of green chlorite, as well as small flakes and frayed laminae of sericite. Leucoxene/rutile occurs as fine-grained turbid aggregates likely derived from a precursor titaniferous mineral (titanite); titanite occurs as small grains and aggregates aligned within the foliation; and magnetite is present as small euhedral crystals of cubic morphology about ~0.2–0.4 mm in size. Traces of hematite form small replacement zones within some magnetite crystals. Pyrite occurs as rare euhedral crystals, and chalcopyrite forms rare, tiny, disseminated angular grains. Zircon is observed as small stubby prisms. Carbonate (calcite) occurs as minor fine-grained granular aggregates (Fig. 4 B).

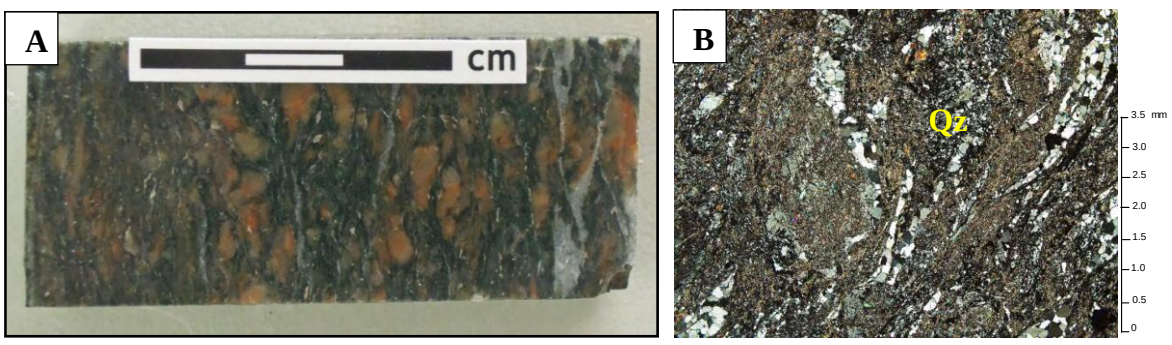


Figure 4: (A) Photograph and (B) photomicrograph of tonalite.
Qz: quartz

4.1.2.3. Biotite Granites

To the naked eye, these granitic rocks from Hiré occur as massive or foliated facies, greenish-gray to pinkish in color, and rich in feldspars. They frequently exhibit deformed textures, sheared zones, and micro-fractures sealed by calcite or quartz (Fig. 5 A).

Under the microscope, the original magmatic texture is strongly modified by low-grade metamorphism (greenschist facies) and ductile deformation. The rock displays mosaics of recrystallized quartz, new plagioclase, as well as flakes of biotite, chlorite, and sericite. These assemblages are accompanied by magnetite, hematite, and sulfides, with r

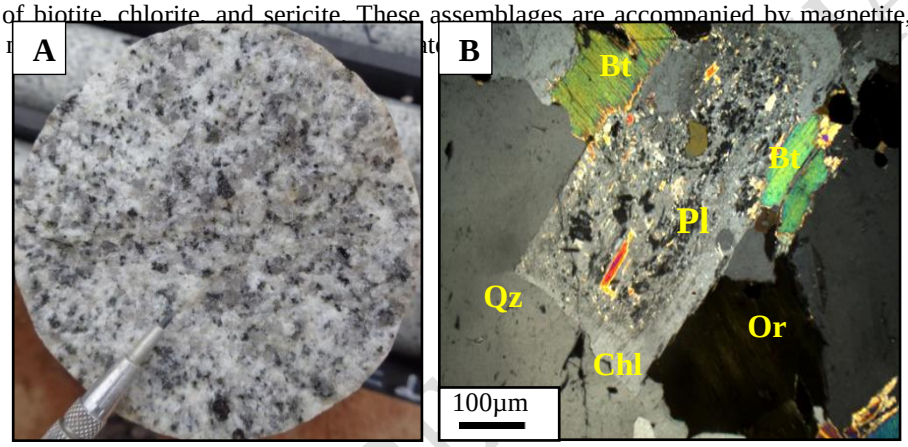


Figure 5: (A) Photograph and (B) photomicrograph of biotite granites.
Pl: plagioclase; Qz: quartz; Or: orthoclase; Bt: biotite; Chl: chlorite.

4.1.3. Dioritoids

The Chappelle dioritoids, although less abundant than the granitoids, are mainly represented by diorites and quartz diorites.

4.1.3.1. Diorite

The dark-colored diorite crystallized as a coarse-grained, massive intermediate magmatic rock, composed of plagioclase + unidentified ferromagnesians + traces of other minerals (Ti-mineral, zircon). No primary magmatic quartz nor residual magmatic quartz was observed; thus, rocks previously considered granodioritic during earlier field works are here interpreted as being of dioritic composition (Fig. 6 A).

In polished thin section, this sample exhibits a partially preserved igneous texture, modified by partial recrystallization and alteration effects (Fig. 6 B).

Plagioclase is moderately abundant. A significant amount of plagioclase occurred as large, stubby prismatic grains generally measuring between approximately 2 and 4 mm. All have undergone advanced replacement by a new optically continuous plagioclase, dotted with small, randomly oriented flakes of sericite.

The rock matrix is composed of a range of minerals forming a foliated felted texture enveloping the large, stubby plagioclase prisms. Plagioclase is moderately abundant, forming small anhedral equant grains that constitute a microgranular mosaic. Chlorite forms small, pleochroic green flakes: some are distributed across the fine-grained plagioclase mosaic as foliated flakes; others occur as denser, chlorite-rich aggregates aligned within the foliation and appear to represent sites of deformed and altered ferromagnesian grains. Sericite forms small, colorless flakes aligned within the foliation. Quartz is present in moderate amounts as small anhedral grains concentrated in weakly elongated granoblastic aggregates parallel to the foliation trace; these quartz aggregates appear to represent weakly deformed primary interstitial quartz grains, rather than quartz phenocrysts. Carbonate (calcite) forms small grains and aggregates, locally aligned in the foliation. Magnetite is present in minor amounts as small euhedral cubic crystals about ~0.1–0.2 mm in size, which tend to be weakly concentrated along certain foliation planes, and rarely within the sites of large altered plagioclase prisms. Rutile occurs as tiny granules

occupying rhomb-shaped crystal sites about ~0.4 mm in size, most likely representing titanite crystals altered to rutile. Pyrite is observed as anhedral grains elongated parallel to the foliation trace, and some grains contain tiny inclusions of chalcopyrite. Zircon occurs as rare small crystals (Fig. 6 A).

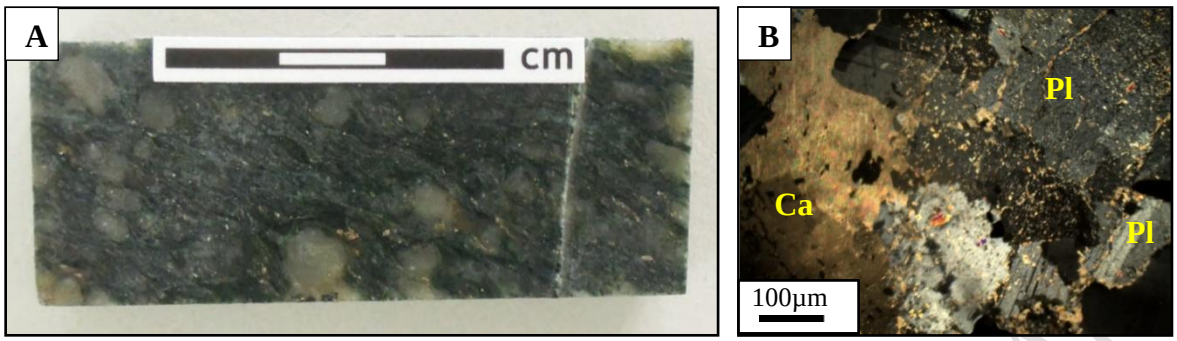


Figure 6: (A) Photograph and (B) photomicrograph of diorite.
Pl: plagioclase; Ca: Calcite.

4.1.3.2. Quartz Diorite

The quartz diorite (Fig. 7) contains a minor amount of additional quartz (7%).

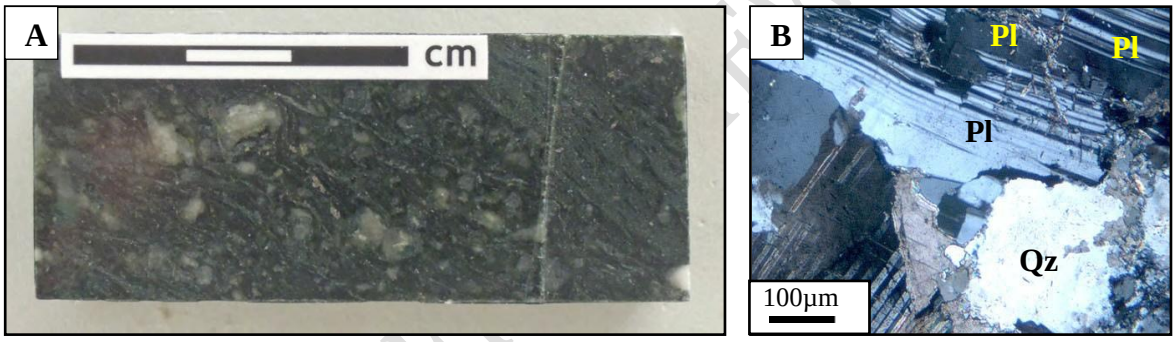
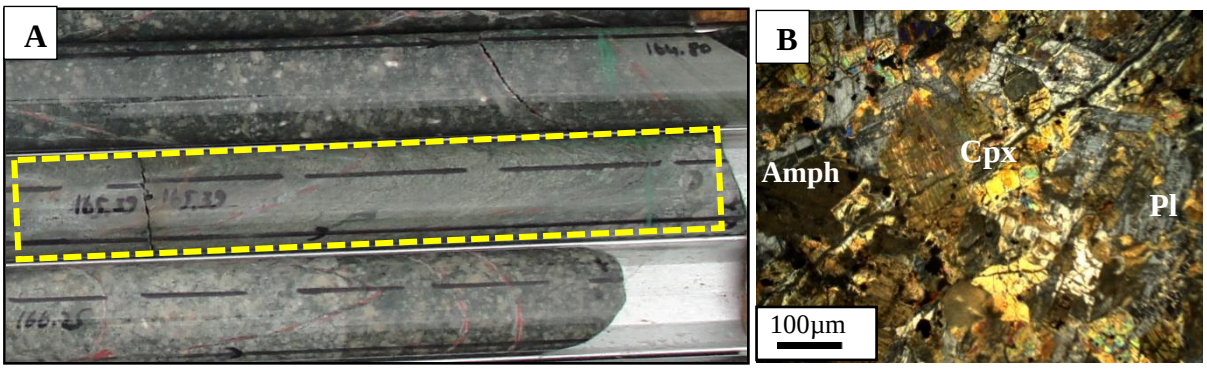


Figure 7: (A) Photograph and (B) photomicrograph of quartz diorite.
Pl: plagioclase; Qz: quartz.

4.1.6. Felsic Dykes

The felsic dykes represent late magmatic manifestations that systematically crosscut the older Birimian metavolcanic and granitoid sequences in the Oumé-Hiré district. These narrow and linear vein-like bodies are genetically and chronologically linked to the late-Eburnean plutonic and hydrothermal evolution of the Fettékro belt.

At the macroscopic scale, these dykes, represented by microgranodiorites, exhibit metric to decametric thicknesses and display a characteristic light mesocratic color (light gray to yellowish due to alteration) (Fig. 8 A). Under the microscope, they display fine aplitic textures or, more frequently, porphyritic textures characterized by quartz and plagioclase phenocrysts (3 to 5 mm) dispersed within a microcrystalline quartzofeldspathic matrix (Fig. 8 B). Field geometric relationships indicate that their emplacement was strongly controlled by the pre-existing fracture network and regional shear zones, preferentially aligning parallel to sub-parallel to the major NE-SW structural grain.



UNDER PEER REVIEW IN IJA

Figure 8: Photograph and photomicrograph of basalt to biotite granites.
Pl: plagioclase; Cpx: Clinopyroxène; Amph: Amphibole.

4.2. Deformation

Most of the structural observations were conducted on drill core samples. Consequently, quartz veins globally oriented N087° were observed, along with an intense foliation trending N100° observed across all felsic and mafic rocks. On average, the contacts between these different lithologies exhibit the same orientations as the foliations.

The rose diagram in Figure 9 shows that all major foliations and veins are globally oriented E-W.

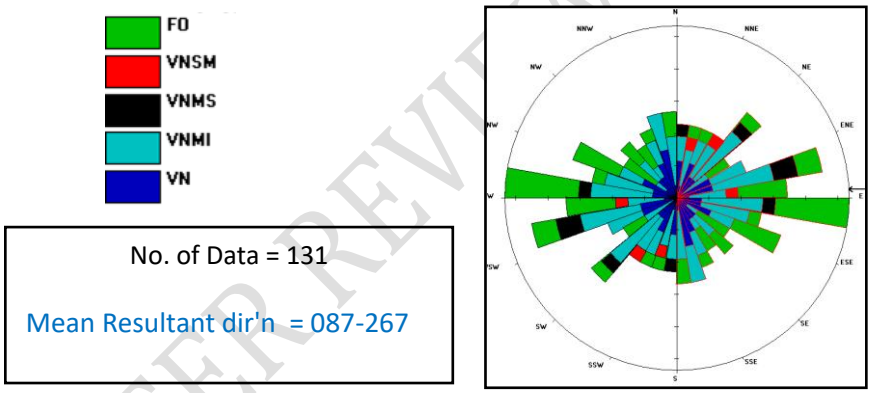


Figure 9: Rose diagram showing the major orientations of foliations and quartz veins.
Fo: Foliation; VNSM: Smoky quartz vein; VNMS: Brecciated quartz vein; VNSM: Milky quartz vein; VNMS: Undifferentiated quartz vein.

4.3. Hydrothermal Alteration

4.3.1. Sericitization

This alteration generally affects the felsic intrusive rocks. It is characterized by the partial or total replacement of feldspars and/or biotite by sericite. The sericitized rock displays a yellowish to greenish color. Sericite, together with silica, forms the alteration mineral assemblage associated with the gold mineralization at the Hiré-Chapelle prospect (Fig. 10).

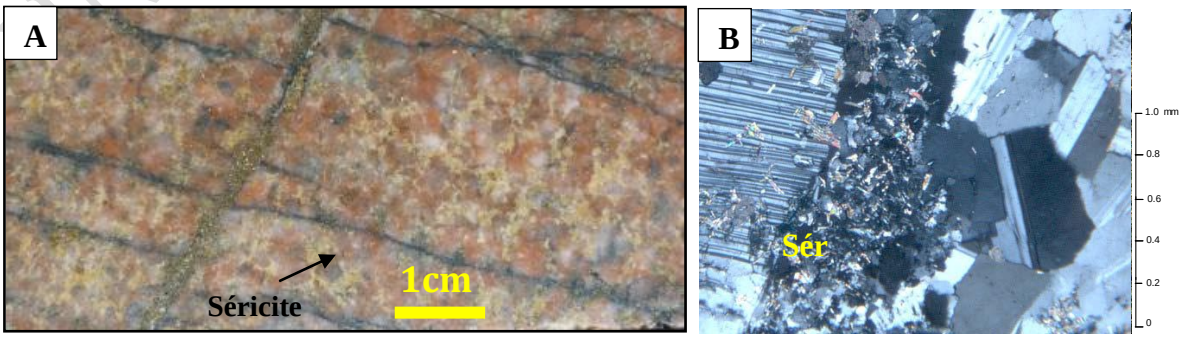


Figure 10: (A) Photograph and (B) photomicrograph showing sericitization in yellow within a granodiorite.
Ser: Sericite.

4.3.2. Silicification

UNDER PEER REVIEW IN IJAR

One of the most widespread alteration types, this is characterized by a significant secondary addition of silica, generally in the form of quartz, within the altered rock. The silicified rock appears as if embedded in a more or less glassy matrix depending on the intensity of the silica alteration n (Fig. 11).

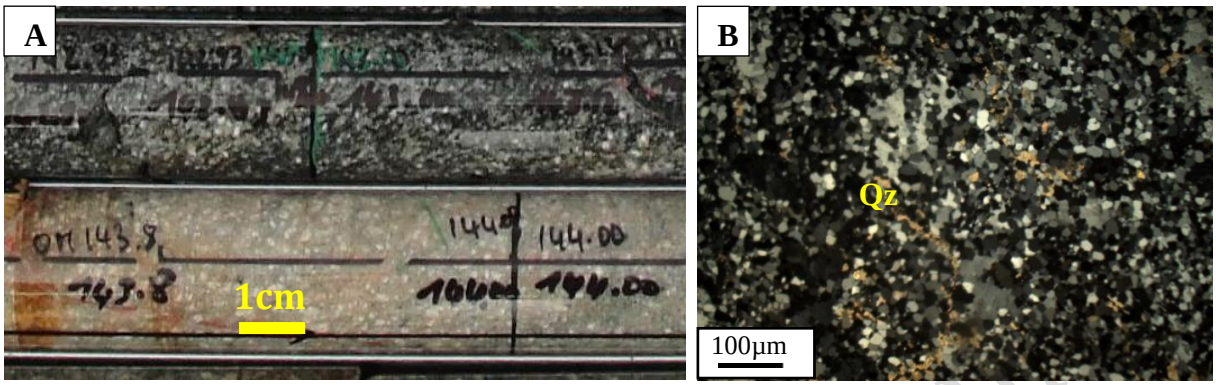


Figure 11: (A) Photograph and (B) photomicrograph showing silica alteration in a granodiorite. *Qz: quartz.*

4.3.3. Carbonatization

Carbonatization is present at Hiré-Chapelle through calcite, ankerite-dolomite, and ankerite-sericite alterations. These carbonates very frequently occur as veinlets (Fig. 12).

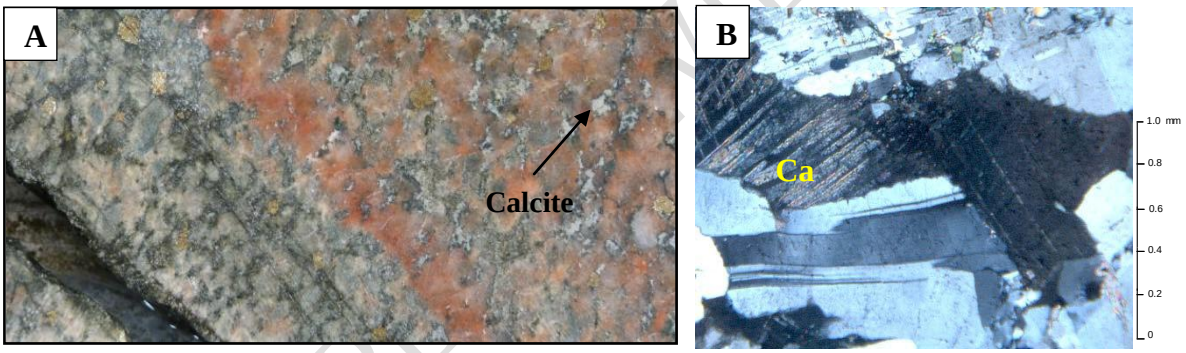


Figure 12: (A) Photograph and (B) photomicrograph showing carbonatization in a granodiorite. *Ca: Calcite.*

4.3.4. Chloritization

This results from the alteration of ferromagnesian silicates, particularly biotite. The chloritized rock appears greenish with chlorite flakes. Chlorite is a characteristic mineral of greenschist-facies (epizonal) metamorphism. Because our study area belongs to the Birimian greenschist facies, chlorite is ubiquitous (Fig. 13).

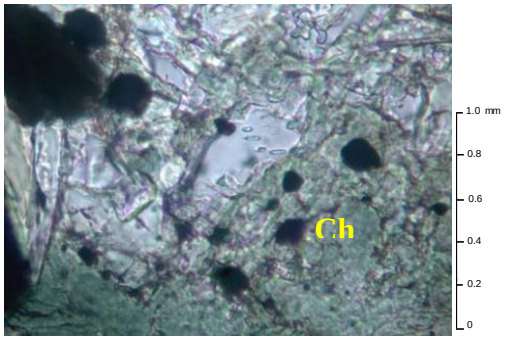


Figure 13: Photomicrograph showing chloritization (greenish coloration) in a granodiorite. *Ch: Chlorite.*

UNDER PEER REVIEW IN IJ

4.3.5. Hematization or pink alteration

Hematite is one of the most abundant minerals on Earth and in the shallow crust. It is an iron oxide with a chemical composition of Fe_2O_3. It is a mineral found in sedimentary, metamorphic, and igneous rocks distributed worldwide. Hematite occurs as a primary mineral and as an alteration product (red or pink coloration) of igneous, metamorphic, and sedimentary rocks. It can crystallize during magma differentiation or precipitate from hydrothermal fluids migrating through a host rock. It can also form during contact metamorphism when hot magmas react with adjacent wall rocks (Fig. 14).

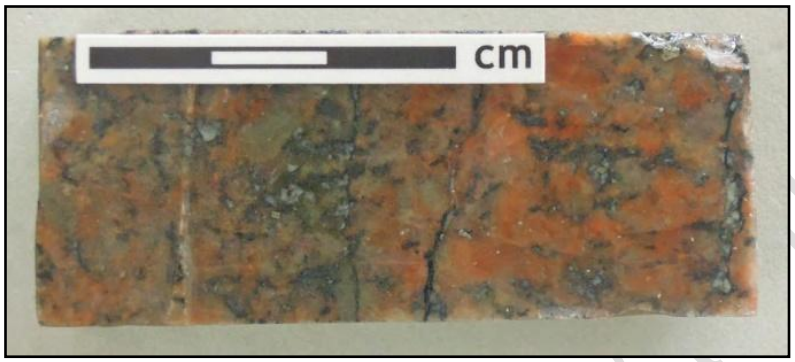


Figure 14: Photograph showing hematization characterized by the red color in a granodiorite.

4.3.6. Albitization or albitic alteration

Feldspar metasomatic albitization is a relatively common phenomenon across a range of geological environments, ranging from hydrothermal to diagenetic settings, and involves the replacement of pre-existing feldspar by virtually pure albite. In the field, albitization fronts can extend perpendicular to fractures and are sometimes recognized by the reddening of feldspars due to hematite nano-inclusions forming within the albite. To determine the mechanism of albitization within plagioclase single crystals: the albite contains fine-grained mica (sericite), often associated with pores, along with hematite precipitates. The chemical interface between plagioclase and albite is sharp on the scale of tens of nanometers, and the crystallographic orientations of the plagioclase and albite coincide to within less than a degree (Fig. 15).

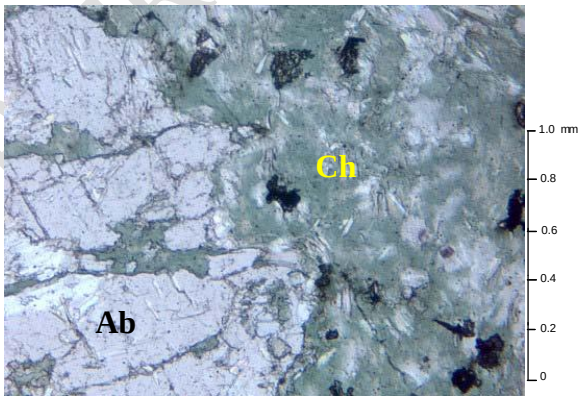


Figure 15: Photomicrograph showing albitization (albitic alteration) in a granodiorite.
Ab: Albite; Ch: Chlorite.

4.4. Metallogeny

In view of this complexity, we relied on lithostructural analysis and gold assay results to better identify the characteristics of the mineralization. High gold grade zones, associated with the lithological and structural features identified in the description, allow for correlations to be established.

4.4.1. Description of Mineralized Zones

In drill hole S1 (Fig. 16 A), the highest gold grades are recorded within the granodiorite between 55 m and 100 m depth and are linked to a smoky quartz vein. The highest grades (4.90 g/t, 4.70 g/t, 4.3 g/t) are generally distributed along the hanging wall and footwall of the quartz vein. This mineralized zone is associated with

UNDER PEER REVIEW IN IJAR

silicification, sulfidation, calcitization, sericitization, and hematization. Drill hole S1 also shows mineralization localized within the saprolite at a depth of 42 m, linked to silicification and sulfidation, with gold grades of approximately 1 g/t. Drill hole S1 exhibits the characteristics of disseminated mineralization (Fig. 16 A).

The main mineralization in drill hole S2 (Fig. 16 B), yielding 7 g/t, is located within a brecciated quartz vein crosscutting the granodiorite at a depth of 100 m. Drill hole S2 also shows disseminated mineralization at respective depths of 25 m and 40 m, with grades of 2.2 g/t and 2.80 g/t. All these mineralized intervals are associated with intense silicification, sulfidation, sericitization, calcitization, and hematization. The oxidation zone exhibits a grade of 1.2 g/t at a depth of 11 m, undoubtedly due to the presence of sulfide-bearing quartz veinlets. Drill hole S2 displays the characteristics of vein-type (lode) mineralization (Fig. 16 B). The diorite, on the other hand, is barren.

Thus, we are able to establish the relationship between lithology, deformation, hydrothermal alteration, and mineralization.

4.4.2. Role of Hydrothermal Alteration

Drill core intervals displaying the highest gold grades are confined to the zone where silicification, carbonatization, sulfidation, and sericitization overlap (Fig. 16 A). However, moving away from the mineralized zones, an increase in chlorite and epidote proportions is observed, accompanied by a decrease in quartz-carbonate-sericite-pyrite proportions. Carbonatization, silicification, sulfidation, and sericitization are the most prominent alteration phenomena at Chappelle, and to a lesser extent, chloritization, epidotization, and

UNDER PEER REVIEW IN IJAR

hematization.

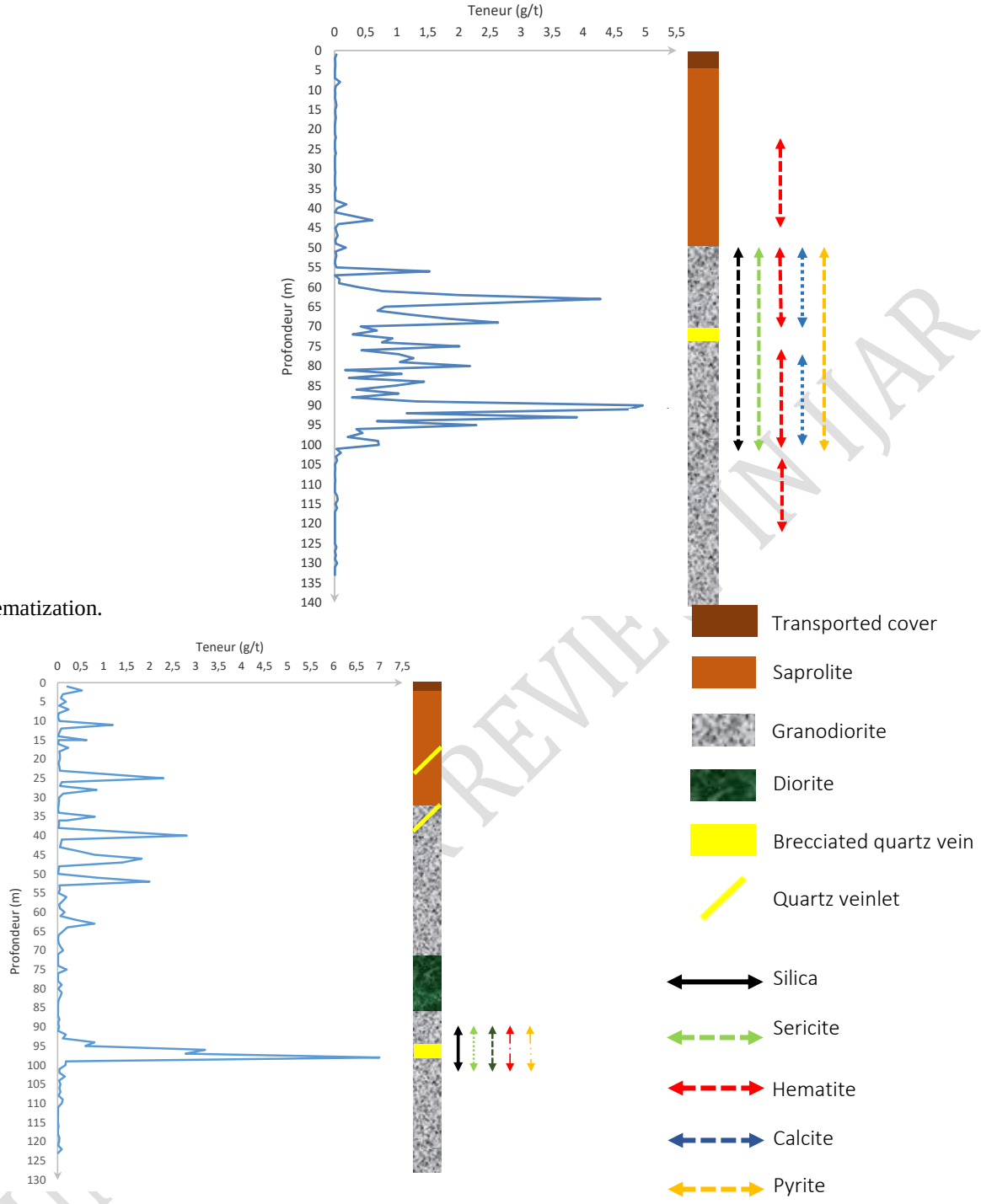


Figure 16: Evolution of gold grade along drill hole (A) S1 and (B) drill hole S2.

5. Discussion

5.1. Metallogenic Model and Characterization of Bimodal Gold Mineralization at the Chapelle Prospect

The integration of petrological, microstructural, metasomatic, and metallogenic data obtained from the Chapelle prospect (Hiré district, southern sector of the Paleoproterozoic Oumé-Fettékro Birimian greenstone belt) allows for the reconstruction of a coherent genetic model characterized by bimodal gold mineralization. This system closely associates a disseminated mineralization style with a lode (vein-type) style, fitting fully within the

geodynamic framework of Paleoproterozoic mesothermal orogenic gold deposits of the West African Craton (WAC) (Milési et al., 1989, 1992 ; Goldfarb et al., 2001, 2005).

5.2. Typology, Petrography, and Expression of Bimodal Mineralization

Systematic drill core analysis (specifically S1 and S2) highlights two complementary precious metal trapping modes, strongly conditioned by the host lithological facies and their mechanical behavior:Disseminated Mineralization (S1-type Facies) : This style is preferentially developed in the core of felsic to intermediate intrusive bodies (granodiorites, interstitial quartz tonalites, and quartz diorites), as well as in the saprolite and peri-lode ductile shear corridors. Gold is distributed sub-homogeneously as fine microscopic grains (10 to 50 μm) within the silicate matrix. It is intimately linked to diffuse sulfidation (xenomorphic to sub-automorphous pyrite $\pm$ chalcopyrite) and a contiguous metasomatic alteration halo combining intense sericitization, carbonatization (calcite, ankerite), silicification, and albitization. Gold grades recorded in these intervals are moderate to medium, generally ranging between 1.00 and 2.80 g/t Au.Lode Mineralization (S2-type Facies) : This high-grade facies (reaching 4.90 to 7.00 g/t Au) is directly controlled by a dense network of cataclastic smoky quartz veins, stockwork veinlets, and hydrothermal breccias. These veins, predominantly trending E-W (N087°–N090°) and ENE-WSW to NNE-SSW (N067.5°), crosscut the intrusive massifs and mafic metavolcanics. Native gold is expressed as inclusions within coarse sulfides (brecciated pyrite, automorphous arsenopyrite), along vein selvedges, or trapped within the open network of reactivation micro-fractures (micro-cataclasis).

5.3. Rheological, Structural, and Metasomatic Controls of the Gold Trap

The genesis and superposition of this dual mineralized facies rely on a triple mechanical, structural, and geochemical convergence:Rheological Competence Contrast (Mechanical Trap) : The injection of dioritic, tonalitic, and granodioritic plutons into a more ductile mafic metavolcanic sequence (pillow-lava metabasalts) created strong rheological heterogeneity during Eburnean compressional phases. Under transpressional stress, the rigid intrusive bodies accommodated deformation through brittle behavior (fracturing, brecciation, and development of sheeted veins), whereas the surrounding metavolcanics absorbed stress via ductile shearing. This contrast maximized secondary permeability at the margins and cores of the intrusions.Polyphase Hydrothermal Drainage (Structural Trap): Regional Eburnean shear corridors (syn- to late D2/D3 deformation) and brittle to brittle-ductile fracturing networks trending N087° and N067.5° acted as major crustal-scale drainage conduits. Episodic fluid pressure fluctuations (fault-valve mechanism, Sibson, 1990) guided the continuous percolation of deep-seated metamorphic-derived fluids (Robert & Poulsen, 2001 ; Groves & Goldfarb, 2018). Metasomatic Geochemical Trap: Reaction between auriferous fluids carrying gold as bisulfide complexes $Au(HS)_2^-$ and the ferromagnesian minerals of the host diorites/metabasalt wall rocks triggered intense wall-rock sulfidation. This chemical destabilization of the bisulfide complexes induced the synchronous precipitation of pyrite, sericite, and native gold (Goldfarb & Groves, 2015).

5.4. Local and Regional Metallogenic Comparisons

The bimodal model recognized at the Chapelle prospect integrates harmoniously into the conceptual framework of orogenic gold deposits within the Birimian domain of West Africa:Local Scale (Oumé-Fettékro Belt and Côte d'Ivoire):Oumé-Hiré District: The bimodal behavior of Chapelle is directly reminiscent of the adjacent deposits of Bonikro, Hiré-Gaza, and Dougbafla (Pouclet et al., 2006; Vidal et al., 2009; Ouattara et al., 2015), where vast envelopes of sericitized and pyritized dioritic/granodioritic intrusions with disseminated mineralization frame high-grade quartz vein structures.Yaouré and Tongon Deposits: Identical couplings between brittle fracturing in competent plutons, perocontiguous sulfidation, and bimodal mineralization control the major reserves of Yaouré (Bessoles, 1977; Kouamelan et al., 2015) and Tongon (Eglinger et al., 2017).Doropo District (Northeast): An identical metallogenic selectivity is observed here, where cataclastic and sericitized smoky quartz hosts the core of the lode mineralization, flanked peripherally by disseminated facies in the wall rocks (Siagné et al., 2022, 2025).Regional Scale (West African Craton):Ashanti Belt (Ghana): Major deposits such as Obuasi exhibit this same dual style, associating very rich quartz-carbonate veins along crustal discontinuities with broad disseminated auriferous metasomatic halos in the host rocks (Allibone et al., 2002; Lawrence et al., 2013).Houndé Belt (Burkina Faso) and Loulo-Gounkoto District (Mali): In the Mana (Burkina Faso) and Loulo (Mali) mines, mineralization associates auriferous quartz stockworks/veins within intermediate-composition intrusions and albitization-sericitization-sulfidation zones bearing disseminated ore (Tarnagda et al., 2024; Royer & Camara, 2025).

6. Conclusion

The gold mineralization of the Chapelle prospect, located in the Hiré district within the Oumé-Fettékro Birimian greenstone belt, constitutes a polyphase mesothermal orogenic system driven by a triple lithological, structural,

UNDER PEER REVIEW IJAR

and metasomatic convergence.The framework of the deposit relies on a mafic metavolcanic sequence (pillow-lava metabasalts) intruded by a differentiated magmatic complex comprising diorites, quartz diorites, tonalites, and granodiorites, all affected by regional greenschist-facies metamorphism. The study highlights a bimodal mineralization nature that combines a disseminated style with medium grades (1.0 to 2.8 g/t Au), characterized by fine gold and disseminated pyrite within sericitized, carbonatized, silicified, and albitized intrusive bodies, and a high-grade lode style (4.9 to 7.0 g/t Au) directly trapped within cataclastic smoky quartz veins, stockworks, and hydrothermal breccias.This gold trapping is governed by the mechanical competence contrast between the rigid intrusive plutons and the ductile volcanic wall rock, by hydrothermal fluid drainage along E-W (N087°) and ENE-WSW (N067.5°) fault structures, as well as by intense wall-rock sulfidation.

References

Abouchami, W., Galer, S. J. G., & Hofmann, A. W. (1990). Pb isotopic systematics of calc-alkaline volcanic rocks from the Paleoproterozoic Birimian of West Africa. *Precambrian Research*, 48(1-2), 115–139.

Allibone, A., McCuaig, T. C., Harris, D., Etheridge, M., Munroe, S., Byrne, D., & Blenkinsop, J. (2002). Lower Proterozoic gold deposits in the Ashanti Belt, Ghana: Geochronological constraints. *Economic Geology*, 97(3), 505–517.

Arnould, M. (1961). Étude géologique des gisements de manganèse de la Côte d'Ivoire. *Mémoires du BRGM*, n° 1, Paris, 235 p.

Bessoles, B. (1977). Géologie de l'Afrique : le Craton Ouest-Africain. *Mémoires du BRGM*, n° 88, Paris, 383 p.

Boher, M., Abouchami, W., Michard, A., Albarede, F., & Arndt, N. T. (1989). Crustal growth in West Africa at 2.1 Ga as deduced from Nd isotopic systematics in Birimian sedimentary rocks. *Journal of Geophysical Research*, 94(B1), 345–359.

Delor, C., Feybesse, J. L., Thieblemont, D., Triboulet, C., & Chevmont, P. (2004). Geological and geodynamical evolution of the Paleoproterozoic Birimian formations of Côte d'Ivoire. *Precambrian Research*, 131(1-2), 45–78.

Doumbia, S., Peucat, J. J., Kouamelan, A. N., Vidal, M., & Lagarde, J. L. (1998). U-Pb geochronology of the Paleoproterozoic domain of Côte d'Ivoire, West African Craton. *Precambrian Research*, 87(3-4), 131–146.

Eglinger, A., Bari, A., Robb, L. J., Augenstine, M., & Zeh, A. (2017). Paleoproterozoic crustal evolution and gold metallogeny of the West African Craton. *Ore Geology Reviews*, 81, 1050–1068. *(Cité dans : 5.4)*

Feybesse, J. L., Ledru, P., Milési, J. P., & Johan, V. (1989). The Paleoproterozoic domains of the West African Craton: A synthesis of structural and metallogenic data. *Precambrian Research*, 44(2), 177–197.

Goldfarb, R. J., & Groves, D. I. (2015). Orogenic gold: Common or evolving fluid and metallogenic sources through time. *Lithos*, 233, 2–26.

Goldfarb, R. J., Groves, D. I., & Gardoll, S. (2001). Orogenic gold and geologic time: A global synthesis. *Ore Geology Reviews*, 18(1-2), 1–75.

Goldfarb, R. J., Baker, T., Dubé, B., Groves, D. I., Hart, C. J. R., & Gosselin, P. (2005). Distribution, character, and genesis of gold deposits in metamorphic terranes. *Economic Geology 100th Anniversary Volume*, 407–450.

Groves, D. I., & Goldfarb, R. J. (2018). Orogenic gold deposits: Past, present and future. *Economic Geology*, 113(1), 1–19.

Groves, D. I., Goldfarb, R. J., Gebre-Mariam, M., Hagemann, S. G., & Robert, F. (1998). Orogenic gold deposits: A proposed classification in the context of their crustal distribution and relationship to other gold deposit types. *Ore Geology Reviews*, 13(1-5), 7–27. *(Cité dans : Introduction)*

UNDER PEER REVIEW IN IJAR

Kouamelan, A. N., Deloule, E., & Peucat, J. J. (2015). Geochronological evolution of the Paleoproterozoic in Côte d'Ivoire. *Journal of African Earth Sciences*, 105, 45–60. *(Cité dans : 5.4)*

Lawrence, D. M., Simmons, S. F., & Seccombe, P. K. (2013). The epithermal-orogenic transition in Archaean/Paleoproterozoic gold deposits. *Mineralium Deposita*, 48(2), 185–201.

Milési, J. P., Feybesse, J. L., Ledru, P., Dommanget, A., Marcoux, E., Egal, E., & Calvez, J. Y. (1989). Les minéralisations d'or du Birimien (Protérozoïque inférieur) de l'Afrique de l'Ouest. Ses relations avec l'évolution lithostructurale et géodynamique. *Chronique de la Recherche Minière*, 497, 3–58.

Milési, J. P., Ledru, P., Feybesse, J. L., Dommanget, A., & Marcoux, E. (1992). Early Proterozoic ore deposits and tectonics of the West African Craton. *Precambrian Research*, 58(1-4), 199–224.

Ouattara, A. S., Coulibaly, I., & Gnanzou, A. (2015). Pétrographie et contexte métallogénique des gisements aurifères de la région d'Oumé-Hiré, Côte d'Ivoire. *Journal of African Earth Sciences*, 110, 112–125.

Pouclet, A., Vidal, M., Alric, G., & Delor, C. (2006). The Paleoproterozoic Birimian terranes of the West African Craton in Côte d'Ivoire: Geology, geochemestry and geodynamics. *Geodinamica Acta*, 19(2), 57–74.

Rapport CENTAMIN (2017). *Geological synthesis and exploration report of the Kalamon permit*. Internal Technical Report, 128 p.

Robert, F., & Poulsen, K. H. (2001). Vein formation and deformation in orogenic gold deposits. *Reviews in Economic Geology*, 14, 111–129.

Sibson, R. H. (1990). Faulting and fluid flow. *Geological Society, London, Special Publications*, 54(1), 69–84.

Siagné, Z. H., Ouattara, A. S., Konan, N. J. J., & Kouamé, F. (2022). New Lithostructural Map of the Doropo Region, Northeast Côte d'Ivoire: Insight from Structural and Aeromagnetic Data. *Journal of African Earth Sciences*, 196, 104680.

Siagné, Z. H., Ouattara, A. S., & Allou, Y. (2025). Integration of airborne gamma-ray spectrometry and remote sensing data for mapping of gold-bearing structures in the Doropo region, Northeastern Côte d'Ivoire. *Geocarto International*, 40(1), 2465074.

Tagini, B. (1971). Esquisse géologique de la Côte d'Ivoire : Note explicative. *SODEMI éd.*, Abidjan, 103 p.

Vidal, M., & Alric, G. (1994). Geodynamic evolution of the Birimian of West Africa. *Precambrian Research*, 67(1-2), 115–130.

Vidal, M., Gosh, P., Pouclet, A., & Delor, C. (2009). The Paleoproterozoic Birimian of Côte d'Ivoire: Volcanism, plutonism and structure. *Journal of African Earth Sciences*, 55(3-4), 145–162.

Yacé, I. (1984). Le Précambrien de la Côte d'Ivoire et l'orogenèse éburnéenne. *Thèse de Doctorat d'État, Université Paris VI*, 420 p. *(Cité dans : 2.1)*

Yao, B. J., Kouamé, F., & Tagini, B. (2001). Contrôles structuraux et lithologiques de la minéralisation aurifère dans le district d'Hiré, Centre-Ouest de la Côte d'Ivoire. *African Journal of Science and Technology*, 2(1), 45–58.

UNDER PEER REVIEW IN IAR